

Spin drift, spin precession, and magnetoresistance in noncollinear magnet/polymer/magnet structures

Z. G. Yu, M. A. Berding, and S. Krishnamurthy
SRI International, Menlo Park, California 94025

(Dated: April 12, 2004)

Abstract

We present a theory to describe spin transport across a polymer sandwiched between magnetic contacts with arbitrary magnetization directions. We find that even a weak magnetic field can significantly modify spin transport in polymers through spin precession. It is shown that the interplay of spin drift (due to electric field) and spin precession can lead to damped oscillating magnetoresistance as the magnetic field increases. Our theory is used to explain the recently observed magnetoresistance and I-V characteristics in such organic structures. Potential device applications are discussed.

PACS numbers: 72.25.Dc, 72.25.Mk, 85.75.Ss, 85.75.Hh

Semiconductor spintronic devices have attracted considerable attention [1] since the discovery of long spin lifetimes in semiconductor structures [2]. Spins in organic materials are expected to last much longer than in inorganic materials because of the vanishing spin-orbit couplings, suggesting that organic materials have significant potential for novel spin devices. Recently strong magnetoresistances have been observed in $\text{La}_{0.7}\text{Sr}_{0.3}\text{MnO}_3$ (LSMO)/sexithienyl (T_6)/LSMO and LSMO/8-hydroxyquinolate aluminum (Alq_3)/Co structures even at room temperature [3, 4]. LSMO is a half-metallic ferromagnet with 100% spin polarization at room temperature [5, 6]. T_6 and Alq_3 are two widely used materials in organic electronics. Theoretical studies of spin-dependent transport in magnet/polymer/magnet structures have just begun [7], and a comprehensive understanding is still lacking. We develop in this paper a theory to describe spin transport and magnetoresistance in these structures. In this theory, the magnetization directions in the two magnets can be arbitrary, and both magnetic-field-induced spin precession and electric-field-induced spin drift are consistently taken into account. The spin precession effect is extremely strong in polymers because of their low carrier mobilities. This theory explains the observed I-V characteristics in LSMO/ T_6 /LSMO [3] and further predicts that the interplay of spin drift and spin precession can give rise to damped oscillating magnetoresistances in magnet/polymer/magnet structures. To date spin transport in noncollinear magnetic structures has been systematically considered only in highly degenerate metallic systems [8, 9], where electric field does not play a role. Semiconductor devices exploiting spin precession have been suggested very recently [10, 11], but a systematic and consistent treatment of spin transport with spin precession is still desirable.

In a magnet/polymer/magnet structure, the magnet work functions and their relative position with respect to the electron- and hole-polaron levels in the polymer determine which type of carrier (electron or hole) is dominantly responsible for transport [12]. We consider a single-carrier device in which the carriers are holes (electron devices can be analyzed similarly), which is appropriate for LSMO/ T_6 /LSMO and LSMO/ Alq_3 /Co structures.

When a voltage is applied to a magnet/polymer/magnet structure, a spin-polarized current is injected into the polymer from the magnets, giving rise to spin accumulation in the polymer. To consider spin precession and noncollinear configurations, where spin accumulation can be along any direction, we use a 2×2 density matrix in spin space to describe the carrier distribution, $\hat{\rho}^P = \rho_0^P \hat{\mathbf{1}} + \hat{\boldsymbol{\sigma}} \cdot \boldsymbol{\rho}^P$. Here $\rho_0^P \hat{\mathbf{1}}$ is the equilibrium carrier distribution of

the nonmagnetic polymer, and $\hat{\boldsymbol{\sigma}} = (\hat{\sigma}_x, \hat{\sigma}_y, \hat{\sigma}_z)$ are Pauli matrices.

The spin-polarized current in the polymer consists of two contributions, drift and diffusion,

$$\hat{\mathbf{j}}^P = \hat{\rho}^P e\nu \mathbf{E} - eD\nabla\hat{\rho}^P, \quad (1)$$

where ν is the carrier mobility and D the diffusion constant in the polymer. Here we neglect the possible magnetic-field effect on the orbital motion (Hall effect), which is reasonable in polymers with low carrier mobilities. In a nondegenerate system, ν and D are connected via Einstein's relation $\nu/eD = 1/k_B T$. The continuity equation for each component of the density matrix in the presence of a magnetic field, \mathbf{B} , reads

$$\frac{\partial\hat{\rho}^P}{\partial t} = -\frac{\hat{\rho}^P - \rho_0^P \hat{\mathbf{1}}}{\tau_S} - \frac{1}{e}\nabla \cdot \hat{\mathbf{j}}^P + \frac{i}{\hbar} \left[\hat{\rho}^P, -\frac{g\mu_B}{2}(\hat{\boldsymbol{\sigma}} \cdot \mathbf{B}) \right], \quad (2)$$

where τ_S is the spin relaxation time g the gyromagnetic factor of the material, and μ_B the Bohr magneton. To emphasize the spin-dependent part in carrier transport, as a simplification, we assume that the charge distribution inside the polymer is homogeneous, and $\nabla\rho_0^P = 0$ and $\nabla \cdot \mathbf{E} = 0$, although a more accurate description requires self-consistently solving Poisson's equation together with transport equations [12]. In steady state we obtain

$$\nabla^2 \boldsymbol{\rho}^P - \frac{e\mathbf{E}}{k_B T} \cdot \nabla \boldsymbol{\rho}^P - \frac{\boldsymbol{\rho}^P}{L^2} - \mathbf{b} \times \boldsymbol{\rho}^P = 0, \quad (3)$$

where $\mathbf{b} \equiv g\mu_B \mathbf{B}/\hbar D$ and $L = \sqrt{D\tau_S}$. This equation provides a consistent description of spin drift and spin precession in polymers. A similar equation for semiconductors was derived recently from the Boltzmann equation [13]. Equation (4) contains \hbar and thus takes account of the quantum feature of spin precession in spin transport. The spin precession effect, controlled by the ratio, \mathbf{B}/D , is particularly important in polymers because of their small diffusion constants (low mobilities).

For systems homogeneous in the lateral direction all quantities depend on only one coordinate (x). We obtain the general solution to Eq. (3) in such a system for a magnetic field

along $\mathbf{B} = B(\sin \theta \cos \phi, \sin \theta \sin \phi, \cos \theta)$,

$$\begin{aligned}
\boldsymbol{\rho}^P(x) &= C_1 \mathbf{v}_0 e^{\lambda_1 x} + C_2 \mathbf{v}_0 e^{\lambda_2 x} \\
&+ C_3 (\mathbf{v}_1 e^{\lambda_3 x} \cos \lambda_4 x - \mathbf{v}_2 e^{\lambda_3 x} \sin \lambda_4 x) \\
&+ C_4 (\mathbf{v}_1 e^{\lambda_3 x} \sin \lambda_4 x + \mathbf{v}_2 e^{\lambda_3 x} \cos \lambda_4 x) \\
&+ C_5 (\mathbf{v}_1 e^{\lambda_5 x} \cos \lambda_4 x + \mathbf{v}_2 e^{\lambda_5 x} \sin \lambda_4 x) \\
&+ C_6 (\mathbf{v}_1 e^{\lambda_5 x} \sin \lambda_4 x - \mathbf{v}_2 e^{\lambda_5 x} \cos \lambda_4 x), \\
\mathbf{v}_0 &= (\sin \theta \cos \phi, \sin \theta \sin \phi, \cos \theta), \\
\mathbf{v}_1 &= (\cos \theta \cos \phi, \cos \theta \sin \phi, -\sin \theta), \\
\mathbf{v}_2 &= (\sin \phi, -\cos \phi, 0), \\
\lambda_{1,2} &= eE/2k_B T \pm \gamma, \\
\lambda_{3,5} &= eE/2k_B T \pm \sqrt{\gamma^2 + \sqrt{\gamma^4 + |\mathbf{b}|^2}/\sqrt{2}}, \\
\lambda_4 &= \sqrt{-\gamma^2 + \sqrt{\gamma^4 + |\mathbf{b}|^2}/\sqrt{2}},
\end{aligned}$$

where $\gamma^2 = (eE/2k_B T)^2 + 1/L^2$. If the magnetic-field-induced spin precession is absent, the general solution becomes $\boldsymbol{\rho}^P(x) = \mathbf{A}_1 e^{x/L_u} + \mathbf{A}_2 e^{-x/L_d}$. Here \mathbf{A}_1 and \mathbf{A}_2 are two constant vectors, and L_u and L_d are the upstream and downstream spin diffusion lengths [14, 15],

$$L_{u,d} = (\pm |eE|/2k_B T + \gamma)^{-1}. \quad (4)$$

The spin transport distance (L_d) is greatly enhanced by the electric field (current).

The two magnets in a magnet/polymer/magnet are described as in Ref. [8, 9]. These magnets can be regarded as magnetic reservoirs in local equilibrium at chemical potentials $\mu_{\mathcal{L},\mathcal{R}}^M$, which is diagonal in spin space $\hat{\mu}_{\mathcal{L},\mathcal{R}}^M = \mu_{\mathcal{L},\mathcal{R}}^M \hat{1}$. Here $\mathcal{L}(\mathcal{R})$ denotes the left (right) magnet. The direction of the magnetization in each magnet is described by the unit vector $\mathbf{m}_{\mathcal{L},\mathcal{R}}$. The current from the left contact to the polymer is [8, 9]

$$\begin{aligned}
\hat{j}^C(0) &= G^\uparrow \hat{u}_{\mathcal{L}}^\uparrow [\hat{\mu}_{\mathcal{L}}^M - \hat{\mu}^P(0)] \hat{u}_{\mathcal{L}}^\uparrow + G^\downarrow \hat{u}_{\mathcal{L}}^\downarrow [\hat{\mu}_{\mathcal{L}}^M - \hat{\mu}^P(0)] \hat{u}_{\mathcal{L}}^\downarrow \\
&- G^{\uparrow\downarrow} \hat{u}_{\mathcal{L}}^\uparrow \hat{\mu}^P(0) \hat{u}_{\mathcal{L}}^\downarrow - G^{\downarrow\uparrow} \hat{u}_{\mathcal{L}}^\downarrow \hat{\mu}^P(0) \hat{u}_{\mathcal{L}}^\uparrow.
\end{aligned} \quad (5)$$

The current from the right contact to the polymer, $\hat{j}^C(d)$, can be written similarly. Here $\hat{\mu}^P$ is the polymer electrochemical potential in the spin space. Operators $\hat{u}_{\mathcal{L}}^{\uparrow(\downarrow)} = \frac{1}{2}[1 + (-)\hat{\boldsymbol{\sigma}} \cdot \mathbf{m}_{\mathcal{L}}]$ and $\hat{u}_{\mathcal{R}}^{\uparrow(\downarrow)} = \frac{1}{2}[1 + (-)\hat{\boldsymbol{\sigma}} \cdot \mathbf{m}_{\mathcal{R}}]$ project spins to the magnetization directions of the magnets.

The above equations can be regarded as a generalized Ohm's law in the spin space. G^\uparrow (G^\downarrow) is the electron conductance in the magnet with spin parallel (antiparallel) to the magnetization direction. $G^{\uparrow\downarrow} = \text{Re}G^{\uparrow\downarrow} + i\text{Im}G^{\uparrow\downarrow}$ is the mixing conductance, which measures the transport capability of spins oriented perpendicular to the magnetization direction. Note that possible interfacial conductances arising from the tunneling barriers between the magnet and the polymer can be included in these spin-dependent conductances. In the diffusive regime G^\uparrow and G^\downarrow can be calculated through $\sigma_c^{\uparrow(\downarrow)}/L_c$, where L_c is length of the contact and $\sigma_c^{\uparrow(\downarrow)}$ is the up-spin (down-spin) conductivity of the contact. It is required that $\text{Re}G^{\uparrow\downarrow} \geq (G^\uparrow + G^\downarrow)/2$ [8].

The electrochemical potential $\hat{\mu}^P$ in the polymer is related to the density matrix $\hat{\rho}^P$. For nondegenerate systems with carriers following the Boltzmann distribution, we find $\hat{\mu}^P = \mu_0^P \hat{1} + \hat{\sigma} \cdot \boldsymbol{\mu}^P$ with

$$\boldsymbol{\mu}^P = \frac{k_B T}{e} \frac{\boldsymbol{\rho}^P}{2|\boldsymbol{\rho}^P|} \left[\ln \left(1 + \frac{|\boldsymbol{\rho}^P|}{\rho_0^P} \right) - \ln \left(1 - \frac{|\boldsymbol{\rho}^P|}{\rho_0^P} \right) \right], \quad (6)$$

and μ_0^P is determined by $d\mu_0^P/dx = -J/\sigma_p = -E$ with σ_p the conductivity of the polymer and $J = \text{Tr}\hat{j}^P$ the total current. Thus $\mu_0^P(x) = -Ex + C_0$, C_0 is a constant.

The requirement that the currents be continuous provides the following boundary conditions: (1) $\hat{j}^C(0) = \hat{j}^P(0)$ and (2) $-\hat{j}^C(d) = \hat{j}^P(d)$. These two 2×2 matrix equations completely determine the eight unknowns – C_i ($i = 0, 1, \dots, 6$) and $\mu_{\mathcal{L}}^M - \mu_{\mathcal{R}}^M$ (voltage drop) – for a given current, J . Having solved these equations, we can calculate the total resistance of the structure $R = (\mu_{\mathcal{L}}^M - \mu_{\mathcal{R}}^M)/J$. All numerical calculations presented here are for room temperature.

The room-temperature conductance parameters appropriate for the LSMO/T₆/LSMO structures can be estimated as follows. In LSMO there is a big gap (~ 1 eV) between up-spin and down-spin conduction bands, and the Fermi energy falls in the up-spin band. Thus $G^\downarrow \ll G^\uparrow$ and $G^\uparrow \simeq \sigma_c/L_c$, where σ_c is the conductivity of LSMO. With $\sigma_c \sim 100(\Omega \text{ cm})^{-1}$ and $L_c \sim 10\mu\text{m}$ in the measured structures, $G^\uparrow \sim 10^5 (\Omega \text{ cm}^2)^{-1}$. The conductance of the polymer is $G_p = \sigma_p/d$. The conductivity of the T₆ sample used in the experiments is $\sigma_p = 10^{-6} (\Omega \text{ cm})^{-1}$. For a 100 nm T₆ film, $G_p \sim 10 (\Omega \text{ cm}^2)^{-1} \ll G^\uparrow$. We then estimate the conductance G^\downarrow from the amplitude of the observed magnetoresistance. Suppose that up-spin and down-spin conduction channels in the polymer are independent for collinear configurations. The total resistance $R \equiv (1/R_{\text{up}} + 1/R_{\text{dn}})^{-1}$, where R_{up} and R_{dn} are the

resistances for up-spin and down-spin channels, respectively. If the magnetizations in the two contacts are parallel, $R_{\text{up}} \simeq 2/G_p$ and $R_{\text{dn}} \simeq 2/G_p + 2/G^\downarrow$. If the magnetizations are antiparallel, $R_{\text{up}} = R_{\text{dn}} \simeq 2/G_p + 1/G^\downarrow$. If the magnetoresistance $\Delta R/R$ is set to 50% (ΔR is resistance difference between the parallel and antiparallel configurations and R the resistance of the antiparallel configuration), similar to the experimental values (30 – 40%), G^\downarrow is estimated to be $10^{-2} \Omega\text{cm}^2$. Therefore $G^\downarrow/G^\uparrow = 10^{-7}$, which is consistent with the band structure of LSMO. $G^{\uparrow\downarrow}$ is set $0.7 \times 10^5 \Omega \text{ cm}^2$ and as we will show later, the results are not sensitive to $G^{\uparrow\downarrow}$ when $\text{Re}G^{\uparrow\downarrow} \geq (G^\uparrow + G^\downarrow)/2$. The intrinsic spin diffusion length in the polymer L is chosen to be 50 nm, similar to the value obtained from the magnetoresistance measurements at weak electric fields [4], which is considerably smaller than the value measured at strong electric fields (~ 150 nm) [3], consistent with Eq. (4).

First we examine spin transport in the absence of spin precession. In Fig. 1(a), we depict the device resistance R as a function of relative angle Θ between the contact magnetizations ($\cos \Theta = \mathbf{m}_{\mathcal{L}} \cdot \mathbf{m}_{\mathcal{R}}$) in the weak electric field regime. The device size, $d = 10$ nm, is much smaller than the spin diffusion length. We see that the device resistance dramatically increases as the relative orientation of the two magnets changes from parallel to anti-parallel. The total resistance for noncollinear configurations also depends on $G^{\uparrow\downarrow}$, but this dependence becomes negligible when $\text{Re}G^{\uparrow\downarrow} \geq (G^\uparrow + G^\downarrow)/2 = 0.5 \times 10^5 \Omega \text{ cm}^2$.

Figure 1(b) shows R as a function of Θ for a device with $d = 200$ nm. When the electric field is weak, the injected carriers from the left LSMO contact become unpolarized when they reach the right contact because $L_d \simeq L = 50 \text{ nm} \ll d$, and therefore the resistance does not depend on magnetization directions of the right LSMO contact. With increase of the electric field, we see that the total resistance becomes sensitive to the magnetization directions of the LSMO contacts, which is due to the field-enhanced spin transport distance in the polymer (L_d) that enables carriers to retain their spin polarization when they reach the right LSMO contact.

We calculate the I-V characteristics of noncollinear structures to interpret the magnetoresistance measurements in LSMO/T₆/LSMO [3]. A theoretical explanation of data for LSMO/Alq₃/Co requires a careful description of the “ill-defined” organic layer adjacent to Co [4] and will be presented elsewhere. The results for LSMO/T₆/LSMO are illustrated in Fig. 2. Experimentally, at zero magnetic field (down-triangles for $d = 140$ nm and circles for $d = 400$ nm) Θ is random, while at a large magnetic field (up-triangles for $d = 140$ nm

and crosses for $d = 400$ nm) $\Theta = 0$. From Fig. 2, for $d = 140$ nm the I-V curves vary with Θ and the experimental data measured at zero magnetic field fall between the curves corresponding to $\Theta = 90^\circ$ and $\Theta = 180^\circ$. For $d = 400$ nm, the three I-V curves for $\Theta = 0$, 90° , and 180° are on top of one another and no magnetoresistance is expected, as shown by the experimental data. The systematic deviation between the theoretical results and the experimental data for $d = 400$ nm might indicate that the quality of the $d = 140$ nm sample is not identical to that of the $d = 400$ nm sample. The I-V characteristics based on our theory are not linear because of the strong electric-field effects on spin transport, and the nonlinearity will become more pronounced at higher voltages.

Next we investigate the impact of spin precession on spin transport in magnet/polymer/magnet structures. We consider structures with $\mathbf{m}_{\mathcal{L},\mathcal{R}}$ in the y - z plane, and spin precession is created by a transverse magnetic field along the x -direction. It is expected from Eq. (3) that even a weak magnetic field can strongly influence spin transport because of the low mobility in the polymer. Figure 3(a) delineates the device resistance as a function of transverse magnetic field for a device of $d = 10$ nm ($L \gg d$) under a vanishing current ($E = 0^+$). We see that the resistance decreases with the applied magnetic field and that the change is particularly strong for an anti-parallel configuration. In the absence of spin precession, the device resistance is large because either spin species must be the minority spin in one of the contacts for the anti-parallel configuration. With a transverse magnetic field, the spin orientation of carriers will vary over the distance through spin precession, providing a channel connecting the majority spins in the two LSMO contacts thereby reducing the resistance. Another effect of spin precession at weak electric fields (diffusive regime) is the reduction of spin accumulation at the interfaces, which occurs because carriers diffuse along random trajectories, and different trajectories lead to different precession angles. This effect is suppressed at high electric fields (drift regime).

Figure 3(b) shows the resistance of an anti-parallel configuration with $d = 200$ nm as a function of transverse magnetic field at high electric fields. Under these electric fields, the spin transport distance is greatly enhanced by drift, $L_d \gg d$. This explains the strong magnetoresistance even for $L \ll d$. We see that the device resistance displays a damped oscillating behavior as the transverse magnetic field increases, and that the oscillating period is proportional to the strength of the electric field. We can understand the oscillation by noticing that spin drift due to electric field leads to a finite transit time, $\tau_D = d/\nu E$. The

time scale of spin precession is determined by the Lamor frequency, ω_L ($\hbar\omega_L = g\mu_B B$). Thus the peaks of resistance occur when $\tau_D = n\tau_P$ ($n = 1, 2, \dots$), i.e., $B = n2\pi\hbar\nu E/g\mu_B d$ [10]. The damping is due to the reduction of spin accumulation at the interfaces because of spin precession. This oscillating resistance does not exist in a metallic system, where spin drift is negligible ($\tau_D \rightarrow \infty$) [see Fig. 3(a)]. We emphasize that the resistance is extremely sensitive to the transverse magnetic field and the spin transport behavior can be rectified in different ways by controlling the interplay between spin precession and spin drift, suggesting that these structures can be used to make ultrasensitive magnetic magnetometers and versatile field-effect transistors [10, 11, 16].

In conclusion, we have presented a theory to describe spin transport in magnet/polymer/magnet structures. This theory considers both the electric-field-induced spin drift and magnetic-field-induced spin precession and explains the observed magnetoresistance and I-V characteristics in LSMO/T₆/LSMO structures. We have also predicted that the interplay of spin drift and spin precession can give rise to damped oscillating magnetoresistances with the transverse magnetic field in magnet/polymer/magnet structures. This theory provides a general framework to understand spin-dependent transport properties in polymer structures and to design organic spintronic devices and magnetic sensors.

We thank Prof. J. Shi for providing us Ref. [4] prior to publication. This work was partly supported by IRAD from SRI International.

-
- [1] See, e.g., S. A. Wolf *et al.*, *Science*, **294**, 1488 (2001), and references therein.
 - [2] J. M. Kikkawa and D. D. Awschalom, *Nature (London)* **397**, 139 (1999).
 - [3] V. Dediu, M. Murgia, F. C. Matocotta, C. Taliani, and S. Barbanera, *Solid State Commun.* **122**, 181 (2002).
 - [4] Z. H. Xiong, D. Wu, Z. V. Vardeny, and J. Shi, *Nature (London)* **427**, 821 (2004).
 - [5] M. Bowen *et al.*, *Appl. Phys. Lett.* **82**, 233 (2003).
 - [6] M. Cavallini, F. Biscarini, V. Dediu, P. Nozar, C. Taliani, and R. Zamboni, cond-mat/0301101.
 - [7] S. J. Xie, K. H. Ahn, D. L. Smith, A. R. Bishop, and A. Saxena, *Phys. Rev. B* **67**, 125202 (2003).
 - [8] A. Brataas, Yu. V. Nazarov, and G. E. W. Bauer, *Phys. Rev. Lett.* **84**, 2481 (2000).

- [9] D. H. Hernando, Yu. V. Nazarov, A. Brataas, and G. E. W. Bauer, *Phys. Rev. B* **62**, 5700 (2000).
- [10] A. M. Bratkovsky and V. V. Osipov, *Phys. Rev. Lett.* **92** 098302 (2004).
- [11] V. V. Osipov and A. M. Bratkovsky, *Appl. Phys. Lett.* **84**, 2118 (2004).
- [12] See, for example, I. H. Campbell and D. L. Smith, *Solid State Phys.* **55**, 1 (2001).
- [13] Y. Qi and S. Zhang, *Phys. Rev. B* **67**, 052407 (2003).
- [14] A. G. Aronov and G. E. Pikus, *Fiz. Tekh. Poluprovodn.* **10**, 1177 (1976) [*Sov. Phys. Semicond.* **10**, 698 (1976)].
- [15] Z. G. Yu and M. E. Flatté, *Phys. Rev. B* **66**, 201202 (R); **66**, 235302 (2002).
- [16] Z. G. Yu, M. A. Berding, and S. Krishnamurthy (unpublished).

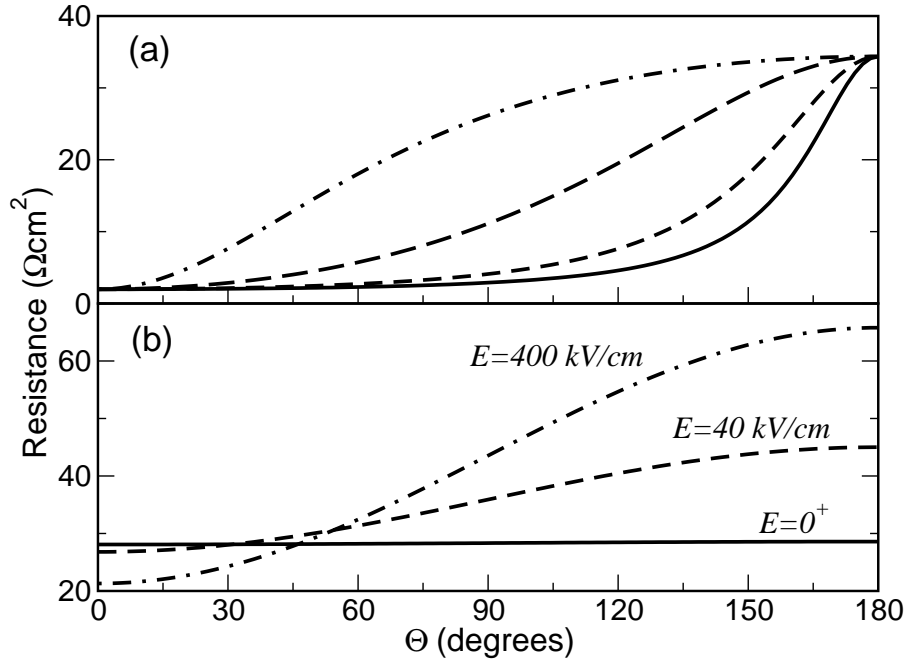


FIG. 1: Total resistance as a function of the angle between the magnetizations of the two LSMO contacts. Panel (a) describes a device of $d = 10$ nm under a vanishing current ($E = 0^+$). Solid, short-dashed, long-dashed, and dot-dashed lines correspond to $G^{\uparrow\downarrow} = 70000, 0.7, 0.07, 0$ (Ωcm^2) $^{-1}$. Panel (b) is for a device of $d = 200$ nm under different currents with the fixed $G^{\uparrow\downarrow} = 70000$ (Ωcm^2) $^{-1}$. Solid, dashed, and dot-dashed lines correspond to $E = 0^+, 40,$ and 400 kV/cm, respectively.

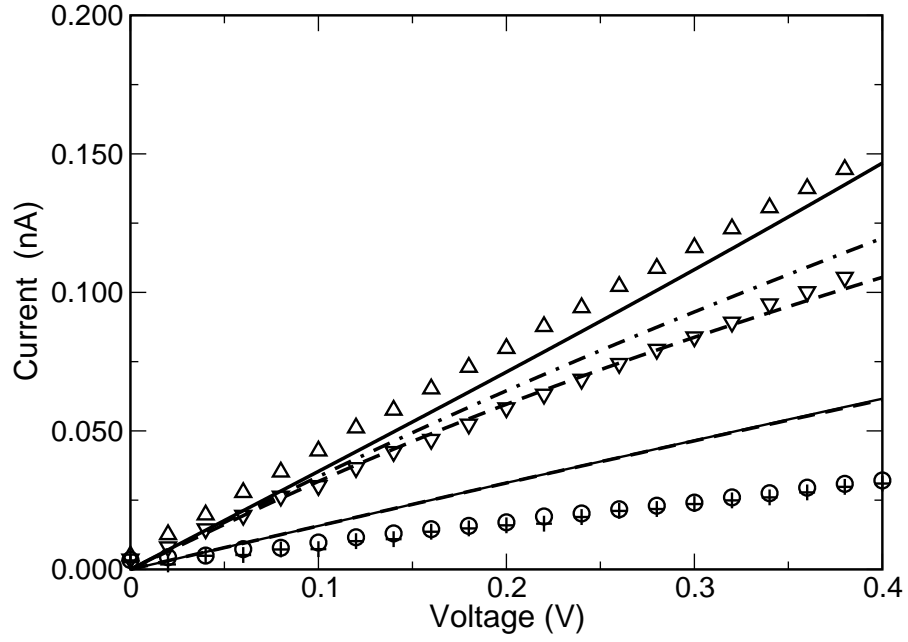


FIG. 2: Total current through noncollinear LSMO/ T_6 /LSMO structures as a function of applied voltage. Solid, dot-dashed, and dashed lines are for $\Theta = 0, 90^\circ$, and 180° , respectively. The upper three lines describe $d = 140$ nm and the lower three lines (which coincide with one another) describe $d = 400$ nm. Symbols are experimental data reported in Ref. [3].

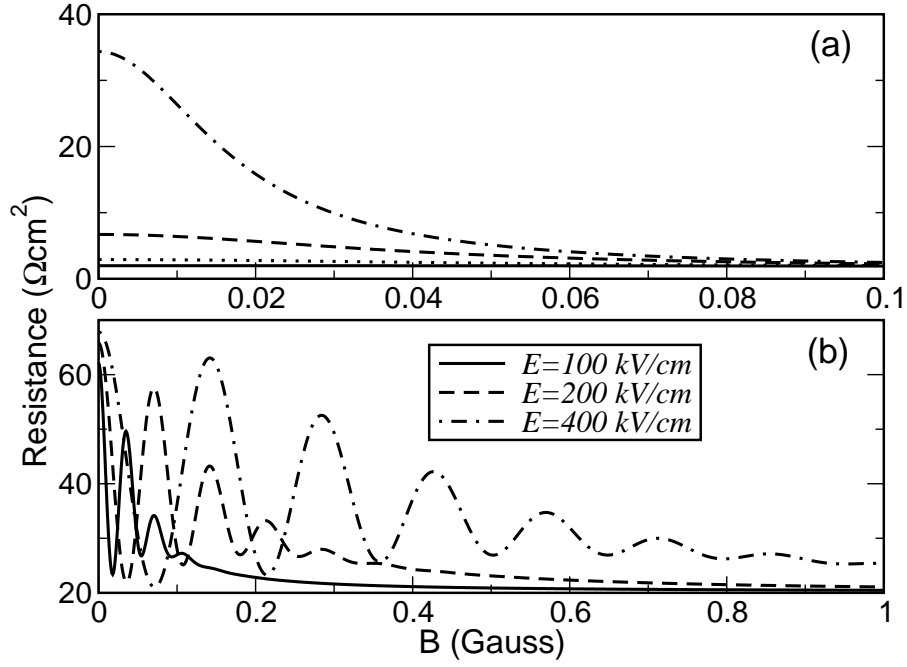


FIG. 3: Total resistance as a function of transverse magnetic field. Panel (a) describes a device of $d = 10$ nm with different Θ under $E = 0^+$. Solid, dotted, dashed, and dot-dashed lines correspond to $\Theta = 0^\circ$, 90° , 135° , and 180° , respectively. Panel (b) describes a device of $d = 200$ nm with $\Theta = 180^\circ$ under different electric fields. Solid, dashed, and dot-dashed lines correspond to $E = 100$, 200 , and 400 kV/cm, respectively. The mobility is set $\nu = 10^{-5} \text{ cm}^2/\text{Vs}$.